

# Scanning Raman Spectroscopy Characterization of 1 Meter Long REBCO Coated Conductor

N Castaneda<sup>1</sup>, G Majkic<sup>2,3\*</sup>, C Goel<sup>2,3</sup>, F C Robles<sup>1,3</sup> and V Selvamanickam<sup>2,3</sup>

<sup>1</sup>Mechanical Engineering Technology, Materials Science and Engineering, University of Houston, Houston, TX 77204, USA

<sup>2</sup>Department of Mechanical Engineering and Texas Center for Superconductivity, University of Houston, TX 77204, USA

<sup>3</sup>Advanced Manufacturing Institute, University of Houston, TX 77023, USA

\*Email: gmajkic@uh.edu

**Abstract.** In this work, we evaluate the use of scanning Raman spectroscopy for characterizing long lengths of REBCO coated conductor tapes, as it can provide detailed insight into structure, composition, and local variations arising from defects or strain. We generate 2D maps of Raman wavelength and intensity features over extended 1 meter length of conductor and correlate them to the information collected by reel-to-reel (R2R) 2D X-Ray Diffraction (2D-XRD) and R2R Scanning Hall Probe Microscopy (SHPM). The three methods are compared in terms of depth of information, detectability of variation in features of interest and the potential for evaluating critical current performance over a range of fields and temperatures.

## 1. Introduction

The advancements in the development and production of REBCO (rare earth, barium, copper, oxygen) coated conductors (CC), also known as second-generation high-temperature superconductors (2G-HTS), have led to a significant increase in their use, particularly in applications such as high energy physics, power transmission lines, particle accelerators and MRI magnets [1-6]. A particularly strong demand for REBCO CCs has been generated by the development of compact fusion power reactor technology where thousands of kilometers of wire are required for magnet fabrication [7]. A recent milestone was achieved by Molodyk et al. [8], who delivered 300 km of REBCO wire for a fusion reactor, which constitutes the largest REBCO CC quantity supplied by a single manufacturer to date. For this project alone, nearly 10000 km of 4mm wide wire is needed, illustrating the extensive amounts of conductor needed for large scale projects. Thus, with the increasing interest in 2G-HTS applications, the demand for large quantities of REBCO tape is expected to increase.

The collective effort of various research groups to understand and enhance the properties of the REBCO (CC) has resulted in remarkable improvement of their performance, particularly in terms of higher critical current under higher magnetic fields. These advancements have been made possible by the incorporation of artificial pinning centers (e.g., [9-13]), as well as increase in REBCO film thickness [14]. However, for large scale production of REBCO, it is crucial to have precise control over the fabrication process to ensure uniformity in properties and performance across the entire length. This brings up the need for high throughput, non-destructive reel-to-reel characterization technique for tape characterization and potentially for closed loop process control if implemented in-line with the deposition system. This allows manufacturers to quickly assess the quality and



uniformity of the tapes, identify any deviations or inconsistencies, and make timely adjustments to optimize the fabrication process.

With the importance of long length characterization in mind, we have developed several operational reel-to-reel systems. One of them is a R2R Two-Dimensional X-Ray Diffraction system (2D-XRD), integrated into an Advanced-Metal Organic Chemical Vapor Deposition (A-MOCVD) system [15] for real-time monitoring and potential integration into process control. The system provides valuable information about the texture, density of pinning centers, strain, film thickness, and insight into  $\text{BaMO}_3$  ( $M = \text{Zr, Hf, Sn, etc.}$ ) pinning efficiency by monitoring the streak angle of BZO (101) reflection in the REBCO tape [15]. The system can either scan linearly along the center of the width or in a zigzag fashion, averaging the signal along both tape width and length directions [15].

For self-field (SF)  $J_c$  characterization, we have developed a R2R Scanning Hall Probe Microscopy (SHPM) [16], first demonstrated in long length R2R fashion by Kiss et al [17, 18]. For in-field  $J_c$ , we have developed an in-field R2R SHPM system operating at 65-77 K and up to 5 T ( $B \perp$  tape) [19]. The obtained 2D spatial distribution maps of  $J_c$  provide insight into tape quality over the entire tape surface and pinning information, with typical speeds of up to 10 and 2 mm/s for the SF and in-field systems, respectively [16] [20]. Additionally, a R2R in-field transport measurement system using the four point I-V measurement method has been built for characterization of long lengths of CC at 65 K and 77 K for magnetic fields up to 5 T applied perpendicular to the tape, with a throughput of 1.2 mm/s [20].

We identify Raman spectroscopy as a promising complementary method both in terms of capabilities in identifying material properties and R2R system implementation. On the identification side, Raman has been demonstrated on REBCO to provide detailed information regarding chemical composition, residual strain, in- and out-of-plane texture, oxygen content, and more [21-28]. In terms of implementation, Raman is non-destructive and easily adaptable for both offline and inline purposes. Raman has been previously employed for characterizing both short REBCO samples and as a R2R tool, both as inline and offline setups using the linear (1D) scanning mode [29-35]. Recently, we have reported on the implementation of a scanning Raman system capable of generating 2D maps [36]. We have demonstrated the proof of concept and 2D Scanning Raman capabilities by mapping short defecting regions previously identified by SHPM [36]. Additionally, we have begun exploring indirect correlations between in-field performance and Raman features [37].

In this manuscript, we aim to evaluate the feasibility of using 2D Raman to scan long lengths of tape in a reel-to-reel (R2R) fashion. One challenge is the speed of the process; while detailed maps like those shown in [36] can be generated for localized defects, scanning hundreds of meters of tape at this resolution is not practical. To address this issue, our study focuses on characterizing 1 meter of tape in a 2D fashion at an intermediate resolution to achieve results comparable to previously reported findings but at an increased throughput. We are currently in the process of building a scanning R2R Raman system, and in this work the aim is to gather information on 1m of tape and evaluate the scanning parameters and level of detail achievable. Furthermore, we compare the Raman results with the information obtained using our R2R SHPM and 2D-XRD scanning tools.

## 2. Experimental

For this study, a 3.6 m segment of REBCO tape that was deposited on Hastelloy/ $\text{Al}_2\text{O}_3$ /IBAD-MgO/Homo-Epi-MgO/LaMnO<sub>3</sub> substrates using the A-MOCVD system was selected [38]. The nominal composition of the tape was  $\text{Gd}_{0.65}\text{Y}_{0.65}\text{Ba}_2\text{Cu}_3\text{O}_{7-\delta} + 0.05 \text{ Zr}$ . This tape segment was chosen due to its significant variation in  $J_c$  along the length, making it suitable for comparing the used characterization techniques. The tape was initially measured by SHPM, scanning across 12 mm width

per mm length resulting in tape speed of  $\sim 0.5$  mm/s. The tape was then measured by R2R 2D-XRD at the same linear speed of 0.5 mm/s with longitudinal resolution of 25 mm. Unlike SHPM and Raman scans that sampled the tape at multiple locations along the width, the 2D-XRD scan was performed in a linear fashion only along the center of the tape width. The source and detector angles were  $12.5$  and  $23.5^\circ$  relative to the tape plane, respectively, and the scan was performed in stationary mode, i.e., without movement of detector or source. The last 1m of the tape was then subjected to 2D Raman scanning.

Raman scanning was conducted on an Xplora Horiba Jobin Yvon confocal micro-Raman spectrometer using a laser 638 nm with power of 0.5mW, and microscope lens (50x/0.75) for a laser spot  $< 2 \mu\text{m}$ . The spectrometer is equipped with an air-cooled CCD detector and  $1200 \text{ cm}^{-1}$  grating. For Raman measurements the 1m tape was sectioned into segments of 30 cm, and precisely aligned on a custom made stage. The maps from each segment were then combined into a continuous 1m map. We chose 1.5 and 1 mm steps along  $x$  and  $y$  (tape length and width, respectively) with acquisition time of 2s per point, with effective scanning speed along the length of tape of  $\sim 0.05$  mm/s. It should be noted that if the same  $x$  resolution as that of 2D-XRD was selected (25 mm), the scan speed would increase to 1.25 mm/s, while still obtaining maps at 11 different  $y$  locations. For linear maps similar to those obtained by 2D-XRD, another order of magnitude in speed increase is possible. The presented data are interpolated on a subgrid of  $1 \times 0.2$  mm along  $x$  and  $y$ . Raman raw spectra were processed using a custom made code that includes cosmic rays and outliers removal [32], background subtraction and Voigt peak fitting. The characteristic wavenumbers and integrated intensities of selected peaks were obtained from these fits.

### 3. Results and Discussion

#### 3.1. 2D-XRD and SHPM $I_c$ 1D Maps

Shown in Figure 1 is a single representative 2D-XRD frame obtained during the inline R2R scan over 3.6 m of tape length. Typically, the selected peaks of interest are REBCO (005), (103), (104),  $\text{RE}_2\text{O}_3$  (004) and BZO (011), and the hastelloy C-276 (111) ring is used for detector calibration. For the present composition, the BZO (011) peak is relatively low. The REBCO peak ratios can be used to detect changes in the structure factor. In this study, we find a strong correlation between SHPM  $I_c$  data and the intensities of REBCO peaks, which is well manifested by the strongest REBCO (005) obtained for this scan.

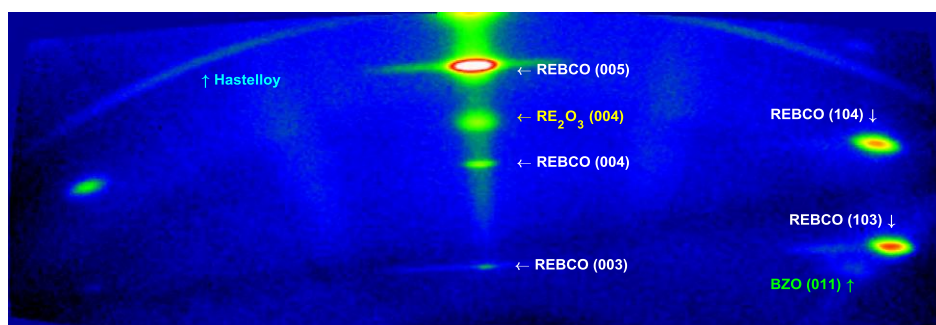


**Figure 1.** Single 2D-XRD frame obtained from R2R scan of 3.6 m long tape. The characteristic peaks tracked as separate regions of interest are indicated with the labels.

Shown in Figure 2 are linear plots of SHPM  $I_c$  and REBCO (005) peak intensity obtained from the 2D-XRD scan. A very good correlation between the two datasets can be observed. The peaks in valleys in SHPM  $I_c$  data are matched by the trend manifested by REBCO (005) peak intensity for the

most part of the 3.6 m scan, as indicated with blue vertical lines for the peaks. The last local minimum in  $I_c$  data at ~3200 mm position is offset from the last minimum for REBCO (005) for unknown reasons, but the curve still follows the  $I_c$  trend. A dropout in SHPM  $I_c$  was also detected by a drop in intensity of REBCO (005) in a related study, where most of the tape exhibited relatively constant current [15]. We also note that the XRD scan did not reveal any significant presence of a-grains along the center of the tape (where the scan was taken), but it did show variation in the ratios of (005), (103) and (104) peak intensities, suggesting changes in structure factor along the length of the tape. While the 2D-XRD dataset can be analyzed in much more detail, for the scope of this study, it can be concluded that the (005) peak intensity clearly captures the trend in  $I_c$ .

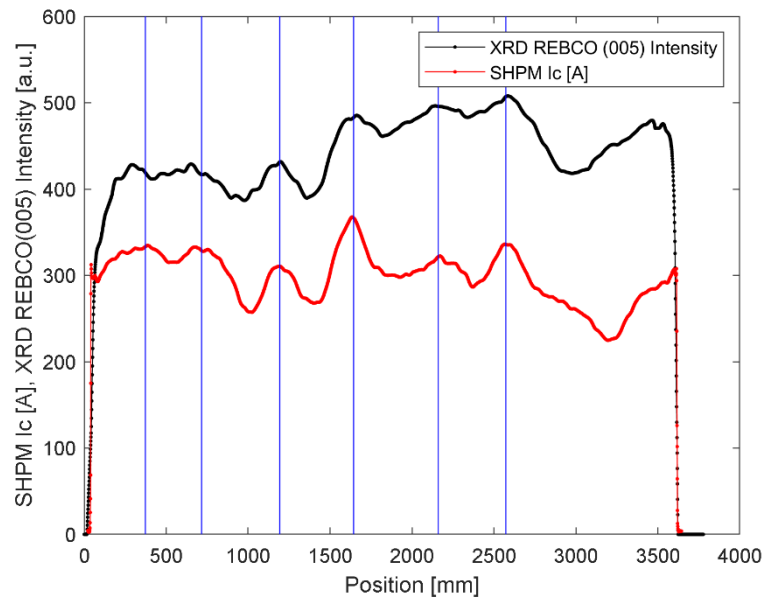


**Figure 2.** SHPM  $I_c$  data and 2D-XRD REBCO (005) peak intensity as a function of tape position. The peaks and valleys in SHPM and XRD data match well for the majority of tape length.

### 3.2. Raman 2D Intensity Maps

Shown in Figure 3 are the intensity maps of the 1 m long and 12 mm wide tape, respectively. In these maps, the characteristic Raman peaks for REBCO conductors are presented. The wavenumber maps were also obtained; however, for the scope of this manuscript we limit our analysis to intensity maps only.

For intensity maps, particular attention should be given to the O2/O3- peak, which is indicative of well-textured c-axis oriented REBCO [33]. This peak is characteristic of both orthorhombic and tetragonal c-axis oriented REBCO [27]. On the other hand, the intensity of O2/O3+ serves as an indication of the amount of tetragonal REBCO domains, especially if Cu2 peak is of higher intensity than Ba peak, as the intensity of Ba peak should be stronger than Cu2 for pure orthorhombic structure [39]. The relative amount of misoriented grains can be examined via O4 peak, as even minor presence of the peak indicates the existence of tilted grains or a-axis oriented grains.

From the 2D intensity maps, one can identify that the maps reveal increased O4 intensity near the edges, while O2/O3- peak intensity is decreased in the same regions. This suggests an increased fraction of a-grains along the edges. Such distribution cannot be accurately determined from 1D integrated plots or linear R2R measurements. The intensity of O2/O3+ peak is low throughout the tape, indicating a well oxygenated film.

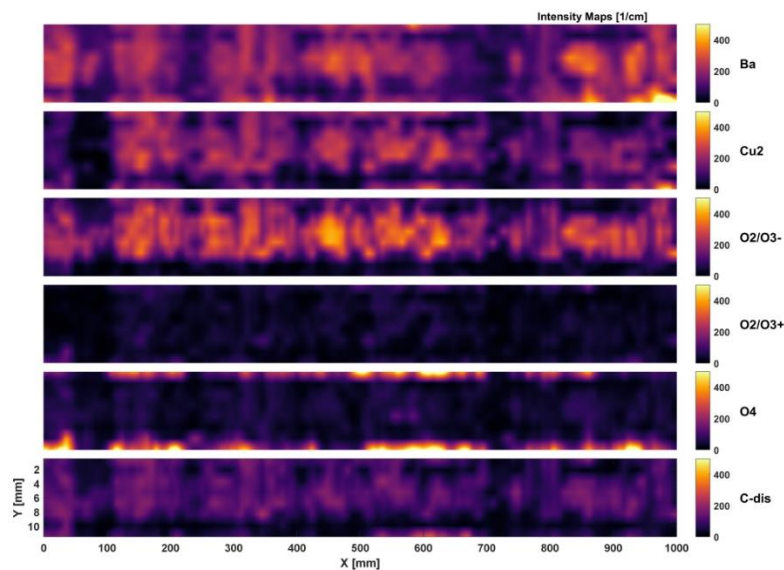


**Figure 3.** Raman Intensity map of characteristic peaks found for REBCO orthorhombic structure. Each map represents a particular peak and the colorbar bar indicates where its intensity is more pronounced along the 1m scanned section.

The intensities of Ba, Cu2 and O2/O3- peaks are varying across the tape, and their trends are compared with SHPM by using integrated intensities across tape width. Shown in Figure 4 is the comparison between SHPM  $I_c$  data and selected Raman intensity features – namely the Ba/Cu2 and O4/(O2/O3-) peak intensity ratios. The first metric can be used as an indication of potential degradation due to oxygen loss [39, 40], while the second metric indicates the relative amount of misoriented grains. The two peak ratios are scaled by arbitrary constants to magnify their variability in the plot to the same scale as the SHPM data. One can observe that the drop in  $I_c$  from SHPM data at ~3200 mm is well matched with both drop in Ba/Cu2 and increase in O4/(O2/O3-) peak intensity ratios. In addition, the peak in  $I_c$  at ~2550 mm coincides with a strong increase in the Ba/Cu2 peak ratio. We note the potential of adding a third metric (in-plane texture) by adding polarized Raman measurements.

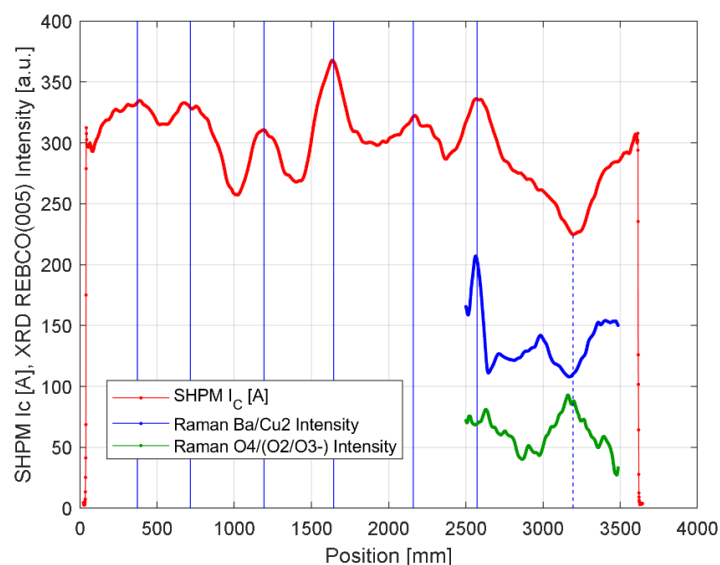


**Figure 4.** Comparison between SHPM  $I_c$  and Raman Ba/Cu2 and O4/(O2/O3-) intensity ratios.

#### 4. Conclusions

In this study, the feasibility of using 2D scanning Raman spectroscopy over long lengths of REBCO coated conductor was investigated. A tape segment of 3.6 m length was characterized by SHPM and 2D-XRD to obtain 1D maps of  $I_c$  distribution and XRD features. The last 1m segment was investigated by scanning Raman spectroscopy to obtain 2D maps of Raman features. The REBCO (005) peak intensity distribution obtained from 2D-XRD correlates well with the  $I_c$  trend measured by SHPM. The Raman 2D intensity maps readily revealed presence of increased fraction of a-axis misoriented grains near both tape edges via O2/O3- and O4 peaks. The Raman intensity profiles integrated over tape width direction were compared with SHPM  $I_c$  distribution as a function of longitudinal tape position. The Ba/Cu2 and O4/(O2/O3-) intensity ratios were found to correlate with a drop in  $I_c$ . The Ba/Cu2 profile was also found to increase at the location of an  $I_c$  peak from SHPM data. The results demonstrate the feasibility of using scanning Raman spectroscopy for both 1D and 2D characterization of long lengths of REBCO tape.

#### 5. References

- [1] Gupta R, Anerella M, Ghosh A, Lalitha S L, Sampson W, Schmalzle J, Kolonko J, Scanlan R, Weggel R, Willen E and Nakao K 2015 Hybrid High-Field Cosine-Theta Accelerator Magnet R&D With Second-Generation HTS *IEEE Transactions on Applied Superconductivity* **25** 1-4
- [2] Tosaka T, Miyazaki H, Iwai S, Otani Y, Takahashi M, Tasaki K, Nomura S, Kurusu T, Ueda H, Noguchi S, Ishiyama A, Urayama S and Fukuyama H 2016 R&D Project on HTS Magnets for Ultrahigh-Field MRI Systems *IEEE Transactions on Applied Superconductivity* **26**
- [3] Ozturk Y, Shen B, Williams R, Gawith J, Yang J, Ma J, Carpenter A and Coombs T 2021 Current Status in Building a Compact and Mobile HTS MRI Instrument *IEEE Transactions on Applied Superconductivity* **31** 1-5
- [4] Koyanagi K, Takayama S, Miyazaki H, Tosaka T, Tasaki K, Kurusu T and Ishii Y 2015 Development of Saddle-Shaped Coils for Accelerator Magnets Wound With YBCO-Coated Conductors *IEEE Transactions on Applied Superconductivity* **25** 1-4
- [5] Himbele J J, Badel A and Tixador P 2016 HTS Dipole Magnet for a Particle Accelerator Using a Twisted Stacked Cable *IEEE Transactions on Applied Superconductivity* **26** 1-5
- [6] Miyazaki H, Iwai S, Otani Y, Takahashi M, Tosaka T, Tasaki K, Nomura S, Kurusu T, Ueda H, Noguchi S, Ishiyama A, Urayama S and Fukuyama H 2016 Design of a conduction-cooled 9.4 T REBCO magnet for whole-body MRI systems *Superconductor Science and Technology* **29**
- [7] Molodyk A and Larbalestier D C 2023 The prospects of high-temperature superconductors *Science* **380** 1220-2
- [8] Molodyk A, Samoilenov S, Markelov A, Degtyarenko P, Lee S, Petrykin V, Gaifullin M, Mankevich A, Vavilov A, Sorbom B, Cheng J, Garberg S, Kesler L, Hartwig Z, Gavrilkin S, Tsvetkov A, Okada T, Awaji S, Abrahimov D, Francis A, Bradford G, Larbalestier D, Senatore C, Bonura M, Pantoja A E, Wimbush S C, Strickland N M and Vasiliev A 2021 Development and large volume production of extremely high current density YBa2Cu3O7 superconducting wires for fusion *Sci Rep* **11** 2084
- [9] Matsumoto K and Mele P 2010 Artificial pinning center technology to enhance vortex pinning in YBCO coated conductors *Superconductor Science and Technology* **23**
- [10] Jha A K and Matsumoto K 2019 Superconductive REBCO thin films and their nanocomposites: The role of rare-earth oxides in promoting sustainable energy *Frontiers in Physics* **7** 1-21
- [11] Li Z, Coll M, Mundet B, Chamorro N, Valles F, Palau A, Gazquez J, Ricart S, Puig T and Obradors X 2019 Control of nanostructure and pinning properties in solution deposited YBa2Cu3O7-x nanocomposites with preformed perovskite nanoparticles *Sci Rep* **9** 5828



- [12] Majkic G, Pratap R, Galstyan E, Xu A, Zhang Y and Selvamanickam V 2017 Engineering of Nanorods for Superior in Field Performance of 2G-HTS Conductor Utilizing Advanced MOCVD Reactor *IEEE Transactions on Applied Superconductivity* **27** 3-7
- [13] Majkic G, Pratap R, Paidpilli M, Galstyan E, Kochat M, Goel C, Kar S, Jaroszynski J, Abraimov D and Selvamanickam V 2020 In-field critical current performance of 4.0  $\mu\text{m}$  thick film REBCO conductor with Hf addition at 4.2 K and fields up to 31.2 T *Superconductor Science and Technology* **33**
- [14] Majkic G, Pratap R, Xu A, Galstyan E and Selvamanickam V 2018 Over 15 MA/cm<sup>2</sup> of critical current density in 4.8  $\mu\text{m}$  thick, Zr-doped (Gd,Y)Ba<sub>2</sub>Cu<sub>3</sub>O<sub>x</sub> superconductor at 30 K, 3T *Scientific Reports* **8** 16-8
- [15] Chen S, Majkic G, Jain R, Pratap R, Mohan V, Goel C and Selvamanickam V 2021 Scale Up of High-Performance REBCO Tapes in a Pilot-Scale Advanced MOCVD Tool With In-Line 2D-XRD System *IEEE Transactions on Applied Superconductivity* **31** 1-5
- [16] Chen S, Li X-F, Luo W and Selvamanickam V 2019 Reel-to-Reel Scanning Hall Probe Microscope Measurement on REBCO Tapes *IEEE Transactions on Applied Superconductivity* **29** 1-4
- [17] Higashikawa K, Guo X, Inoue M, Jiang Z, Badcock R, Long N and Kiss T 2017 Characterization of Critical Current Distribution in Roebel Cable Strands Based on Reel-to-Reel Scanning Hall-Probe Microscopy *IEEE Transactions on Applied Superconductivity* **27** 1-4
- [18] Higashikawa K, Uetsuhara D, Inoue M, Fujita S, Iijima Y and Kiss T 2017 Characterization of Local Critical Current Distribution in Multifilamentary Coated Conductor Based on Reel-to-Reel Scanning Hall-Probe Microscopy *IEEE Transactions on Applied Superconductivity* **27** 1-4
- [19] Li Y, Chen S, Paidpilli M, Jain R, Goel C and Selvamanickam V 2022 A Reel-to-Reel Scanning Hall Probe Microscope for Characterizing Long REBCO Conductor in Magnetic Fields Up to 5 Tesla *IEEE Transactions on Applied Superconductivity* **32** 1-6
- [20] Li X F, Yahia A B, Majkic G, Kochat M, Kar S and Selvamanickam V 2017 Reel-to-reel critical current measurement of REBCO coated conductors *IEEE Transactions on Applied Superconductivity* **27** 4-8
- [21] Zhao P, Ouyang X, Yu J, Xu H, Wang S and Li F 2021 Measurement of Residual Stress in YBa<sub>2</sub>Cu<sub>3</sub>O<sub>7-x</sub> Thin Films by Raman Spectroscopy *Journal of Low Temperature Physics* **202** 382-96
- [22] Maroni V A, Kropf A J, Aytug T and Paranthaman M 2010 Raman and x-ray absorption spectroscopy characterization of Zr-doped MOCVD YBa<sub>2</sub>Cu<sub>3</sub>O<sub>6+ $\delta$</sub>  *Superconductor Science and Technology* **23**
- [23] Lee E, Kim C and Yoon S 2008 Raman Scattering Studies of YBa<sub>2</sub>Cu<sub>3</sub>O<sub>7-x</sub> Coated Conductors *Journal of the Korean Physical Society* **53** 3348-51
- [24] Iliev M N, Hadjiev V G, Jandl S, Le Boeuf D, Popov V N, Bonn D, Liang R and Hardy W N 2008 Raman study of twin-free ortho-II YBa<sub>2</sub> Cu<sub>3</sub> O<sub>6.5</sub> single crystals *Physical Review B - Condensed Matter and Materials Physics* **77** 3-7
- [25] Maroni V A, Li Y, Feldmann D M and Jia Q X 2007 Correlation between cation disorder and flux pinning in the y Ba<sub>2</sub> Cu<sub>3</sub> O<sub>7</sub> coated conductor *Journal of Applied Physics* **102** 1-5
- [26] Thomsen C and Kaczmarczyk G 2006 Vibrational Raman Spectroscopy of High-temperature Superconductors *Handbook of Vibrational Spectroscopy*
- [27] Venkataraman K, Baurceanu R and Maroni V A 2005 Characterization of MBa<sub>2</sub>Cu<sub>3</sub>O<sub>7-x</sub> thin films by Raman microspectroscopy *Applied Spectroscopy* **59** 639-49
- [28] González J C, Mestres N, Puig T, Gázquez J, Sandiumenge F and Obradors X 2004 Biaxial texture analysis of YBa<sub>2</sub> Cu<sub>3</sub> O<sub>7</sub> -coated conductors by micro-Raman spectroscopy *Physical Rev B* **70** 1-8

- [29] Aytug T, Paranthaman M, Heatherly L, Zuev Y, Zhang Y, Kim K, Goyal A, Maroni V A, Chen Y and Selvamanickam V 2009 Deposition studies and coordinated characterization of MOCVD YBCO films on IBAD-MgO templates *Superconductor Science and Technology* **22**
- [30] Aytug T, Paranthaman M, Specht E D, Zhang Y, Kim K, Zuev Y L, Cantoni C, Goyal A, Christen D K, Maroni V A, Chen Y and Selvamanickam V 2010 Enhanced flux pinning in MOCVD-YBCO films through Zr additions: Systematic feasibility studies *Superconductor Science and Technology* **23** 0-7
- [31] Chen Z, Maroni V A, Miller D J, Li X, Rupich M W and Feenstra R 2010 Examination of through-thickness/through-time phase evolution during an MOD-type REBCO precursor conversion using Raman microscopy *Superconductor Science and Technology* **23** 085006-
- [32] Maroni V A, Reeves J L and Schwab G 2007 On-line characterization of YBCO coated conductors using raman spectroscopy methods *Applied Spectroscopy* **61** 359-66
- [33] Miller D J, Maroni V A, Hiller J M, Koritala R E, Chen Y and Black J L R 2009 Characterization of Long-Length, MOCVD-Derived REBCO Coated Conductors *IEEE Transactions on Applied Superconductivity* **19** 3176-9
- [34] Venkataraman K, Lee D F, Leonard K, Heatherly L, Cook S, Paranthaman M, Mika M and Maroni V A 2004 Reel-to-reel x-ray diffraction and raman microscopy analysis of differentially heat-treated Y-BaF<sub>2</sub>-Cu precursor films on metre-length RABiTS *Superconductor Science and Technology* **17** 739-49
- [35] Venkataraman K, Baurceanu R and Maroni V A 2005 Characterization of MBa<sub>2</sub>Cu<sub>3</sub>O<sub>7-x</sub> thin films by Raman microspectroscopy *Applied Spectroscopy* **59** 639-49
- [36] Castaneda N, Majkic G and Robles F C 2021 Scanning Raman spectroscopy for inline characterization of 2G-HTS conductors *Superconductor Science and Technology* **34**
- [37] Castaneda N, Majkic G, Robles F and Selvamanickam V 2023 Correlation Between Critical Current Density and Raman Spectra of Tetragonal REBCO *IEEE Transactions on Applied Superconductivity* **33** 1-6
- [38] Majkic G, Galstyan E and Selvamanickam V 2015 High Performance 2G-HTS Wire Using a Novel MOCVD System *IEEE Transactions on Applied Superconductivity* **25** 3-6
- [39] Lange K, Sparkes M, Bulmer J, Feighan J, O'Neill W and Haugan T 2020 Analysing laser machined YBCO microbridges using raman spectroscopy and transport measurements aiming to investigate process induced degradation *Lasers in Engineering* **46**
- [40] Li Y B, Shelley C, Cohen L F, Caplin A D, Stradling R A, Kula W, Sobolewski R and MacManus-Driscoll J L 1996 Raman studies of laser-written patterns in YBa<sub>2</sub>Cu<sub>3</sub>O<sub>x</sub> films *Journal of Applied Physics* **80** 2929-34

### Acknowledgments

This work was partly funded by award DE-SC0016220 from the U.S. Department of Energy Office of High Energy Physics. One author (VS) has financial interest in AMPeers.